

Large thermoelectric power factor in TiS_2 crystal with nearly stoichiometric composition

H. Imai, Y. Shimakawa, and Y. Kubo

Fundamental Research Laboratories, NEC Corporation, 34 Miyukigaoka, Tsukuba 305-8501, Japan

(Received 23 August 2001; revised manuscript received 16 October 2001; published 10 December 2001)

A TiS_2 crystal with a layered structure was found to have a large thermoelectric power factor. The in-plane power factor S^2/ρ at 300 K is $37.1 \mu\text{W}/\text{K}^2\text{cm}$ with resistivity (ρ) of $1.7 \text{ m}\Omega \text{ cm}$ and thermopower (S) of $-251 \mu\text{V}/\text{K}$, and this value is comparable to that of the best thermoelectric material, Bi_2Te_3 alloy. The electrical resistivity shows both metallic and highly anisotropic behaviors, suggesting that the electronic structure of this TiS_2 crystal has a quasi-two-dimensional nature. The large thermoelectric response can be ascribed to the large density of states just above the Fermi energy and inter-valley scattering. In spite of the large power factor, the figure of merit ZT of TiS_2 is 0.16 at 300 K, because of relatively large thermal conductivity, $68 \text{ mW}/\text{K cm}$. However, most of this value comes from reducible lattice contribution. Thus, ZT can be improved by reducing lattice thermal conductivity, e.g., by introducing a rattling unit into the inter-layer sites.

DOI: 10.1103/PhysRevB.64.241104

PACS number(s): 72.15.Eb, 72.15.Jf, 81.05.Bx

Thermoelectric energy conversion, which transforms heat directly into electricity, has attracted much interest in recent years for possible applications to “environmentally friendly” electric-power generators and highly reliable, small-scale refrigerators used for electronic devices. The efficiency of a thermoelectric device is defined by its material properties through the dimensionless figure of merit, $ZT = S^2T/\rho(\kappa_e + \kappa_l)$, where S is the Seebeck coefficient, T is operating temperature, ρ is resistivity, and κ_e and κ_l are carrier and lattice thermal conductivities, respectively. Although some thermoelectrics, such as Bi_2Te_3 , are used in particular fields of application, their efficiencies, at the best ZT of about 1, are not enough for wider use in commercial applications. Thus, development of materials with higher efficiency is one of the current main interests in research on thermoelectric materials.

A newly proposed concept, “phonon-glass and electron-crystal” (PGEC), gives us clues to develop new materials with large ZT . PGEC has low thermal conductivity like glass and high electrical conductivity usually observed in crystals. Filled skutterudite antimonides^{1–3} and Ge chalcogenides^{4,5} are newly discovered PGEC. By introducing rattling atoms into parent electrically conductive cage (to make phonon glass state), we can produce large ZT materials. Other examples of PGEC are superlattices,^{6–8} in which the mean free path of heat-carrying phonons is considerably reduced because of their two-dimensional structure. In addition, a theoretical calculation predicted that a two-dimensional electronic structure enhances thermopower,⁹ and such a structure is a great advantage of thermoelectrics. In light of this PGEC concept, conducting compounds with naturally layered structure are candidate materials for thermoelectrics, if they have a large power factor, $\text{PF} = S^2/\rho$. They are expected to have intrinsically low κ_l , like superlattices, and κ_l can be reduced by introducing rattling units into inter-layer sites.

A layered-structure material TiS_2 exhibits metallic conductivity, thus it can be a good thermoelectric material. It has an anisotropic structure with a trigonal space group, $P\bar{3}m1$, as shown in Fig. 1.¹⁰ And it consists of infinite layers of edge-sharing TiS_6 octahedra. In the layers, TiS_6 octahedra are

combined with each other tightly through strong covalent bonds, while each layer stacks weakly by van der Waals force. Transport properties of TiS_2 are strongly affected by its large off stoichiometry.^{11–15} Excess titanium atoms are intercalated into the van der Waals gap, and they introduce electrons into the host TiS_6 layers, giving rise to metallic conductivity with a carrier density of 10^{20} – 10^{21} cm^{-3} . Although the basic transport properties of TiS_2 and their dependence on chemical composition have been extensively studied, the thermoelectric properties of TiS_2 have not been discussed, probably because metallic materials are not suitable for thermoelectrics.

In this study we investigate the electrical, thermal transport, and thermoelectric properties of TiS_2 single crystal with nearly stoichiometric composition, since it is expected to have a more two-dimensional nature than large-off-stoichiometric TiS_2 and, thus, good thermoelectric properties.

A single crystal (dimensions: $10 \times 5 \times 0.1 \text{ mm}^3$) was grown by a chemical-vapor-transport method using I_2 transport agent. In-plane resistivity (ρ_a) and out-of-plane resistivity (ρ_c) were measured by the van der Pauw and Montgomery methods, respectively, using a lock-in technique in the temperature range from 4 to 300 K. Ther-

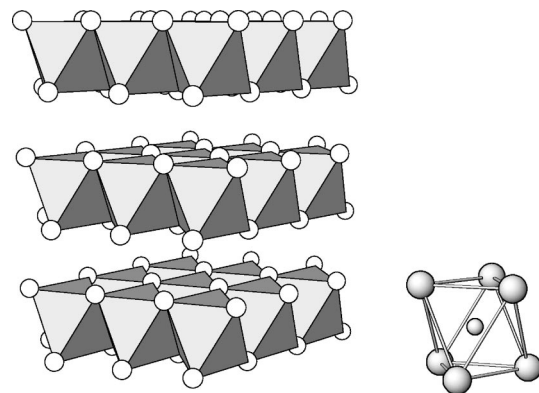


FIG. 1. Crystal structure of TiS_2 (space group $P\bar{3}m1$) and TiS_6 octahedral unit.

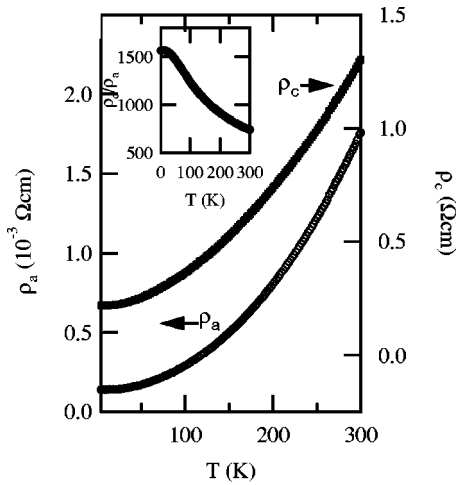


FIG. 2. Temperature dependence of in-plane resistivity, ρ_a , and out-of-plane resistivity, ρ_c . The inset shows the anisotropy ratio, ρ_c/ρ_a .

mopower in this temperature range was measured by the conventional constant ΔT method. In-plane Hall resistivity up to 2 T was measured in the van der Pauw configuration by applying the magnetic field normal to the c plane in the temperature range from 5 to 300 K. In-plane and out-of-plane thermal conductivities at room temperature were measured by the ac thermal diffusivity and the laser flush methods, respectively.

Figure 2 shows the in-plane resistivity ρ_a , out-of-plane resistivity ρ_c , and anisotropy ratio ρ_a/ρ_c . Both ρ_a and ρ_c exhibited metallic behaviors, and they almost depend on T^2 ($\rho_a \propto T^{2.18}$, $\rho_c \propto T^{1.78}$). Figure 3 shows the in-plane carrier density, $n=1/R_H e$ and the inverse Hall mobility $1/\mu_H = \rho/R_H$ as a function of T . The carrier density at room temperature is $2.8 \times 10^{20} \text{ cm}^{-3}$ and almost independent of T . If the Ti^{4+} state is assumed, this carrier density gives the amount of excess titanium to be 0.0001 atoms/f.u., which indicates that the chemical composition of this crystal is very close to the stoichiometry.¹⁶ It is noted here that this carrier density in TiS_2 is still one order of magnitude larger

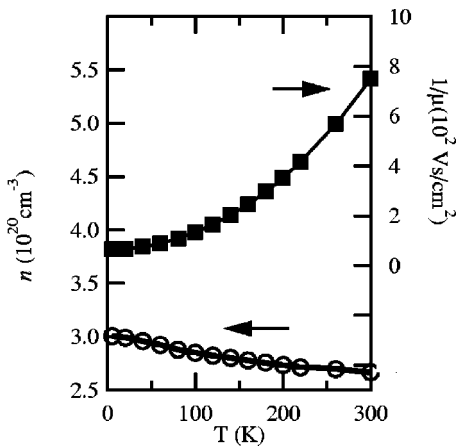


FIG. 3. Temperature dependence of in-plane carrier density and inverse Hall mobility.

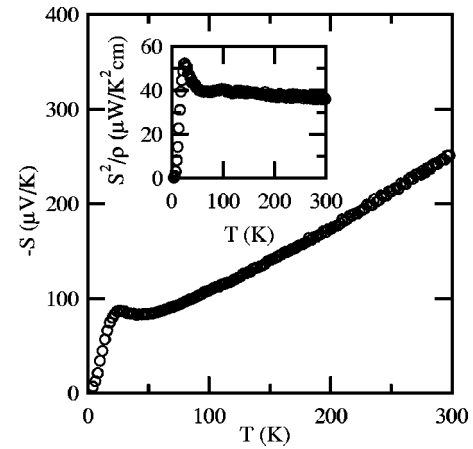


FIG. 4. Temperature dependence of in-plane thermopower. The inset shows the thermoelectric power factor.

than that in thermoelectric Bi_2Te_3 with optimum carrier density.

The resistivity-anisotropy ratios are large: 750 at 300 K and 1500 at 5 K. These ratios suggest that doped electron carriers are confined within the TiS_6 layers, thus, the electronic structure of TiS_2 is quasi-two-dimensional. In-plane Hall mobility strongly depends on T ($1/\mu_H \propto T^{2.14}$) and decreases with increasing T from $150 \text{ cm}^2/\text{V s}$ at 5 K to $15 \text{ cm}^2/\text{V s}$ at 300 K. The significant increase in ρ with increasing T arises from the increase in scattering rate ($\propto 1/\mu_H$). The metal-like temperature dependence of ρ_c in the order of about $1 \Omega\text{cm}$ is quite unusual. Although we cannot explain the dependence of ρ_c on T satisfactorily, the random network of marginally metallic paths along the c axis between the metallic layers can give rise to it.

Figure 4 shows the dependence of in-plane thermopower S on temperature. The thermopower shows a broad peak near 30 K due to the phonon-drag effect resulting from the strong electron-phonon interaction.¹⁷ Above 50 K, S linearly depends on T , and reaches a large negative value, $-251 \mu\text{V/K}$ at 300 K. Since the same order of large S (about $200 \mu\text{V/K}$) has been measured in the $\text{Bi}_2\text{Te}_3\text{-Sb}_2\text{Te}_3$ system with carrier density of $3 \times 10^{19} \text{ cm}^{-3}$, S of $-251 \mu\text{V/K}$ is a surprisingly large value for such a high-carrier-density material.

To understand the above described transport properties, a characteristic electronic structure of TiS_2 should be considered. An electronic band-structure calculation revealed that a primary Ti $3d$ band crosses the Fermi level, making multi-valley structures with six small electron pockets around the L -point in the hexagonal Brillouin zone. In such a multivalley electronic structure, inter-valley scattering significantly contributes to transport properties at higher temperatures, since it requires phonons with a large wave vector (almost half of the Brillouin zone).^{11,18} Taking into account the inter-valley scattering, we can explain the observed nearly- T^2 dependence of ρ_a as discussed in Ref. 11. If we assume simple intra- and inter-valley scattering with acoustic phonons, the inverse of total relaxation time is given by $1/\tau_{\text{total}} = 1/\tau_{\text{intra}} + 1/\tau_{\text{inter}}$. Here, $1/\tau_{\text{intra}}$ linearly changes with T , while $1/\tau_{\text{inter}}$ is roughly proportional to $1/[\exp(\Theta_D/T) - 1]$, where Θ_D is the Debye temperature.¹¹ Thus, the temperature depen-

TABLE I. Thermoelectric and transport properties of single crystalline TiS_2 , Bi_2Te_3 - Bi_2Se_3 , Ge chalcogenides, and Co-based skutterudite antimonides at 300 K. Note that $\text{La}(\text{FeCo})\text{Sb}_3$ and $\text{Yb}_{0.02}\text{Co}_4\text{Sb}_{12}$ have ZT of about 1 at high temperatures.

Sample	ρ (m Ω cm)	S ($\mu\text{V}/\text{K}$)	κ (κ_e) (mW/cm K)	ZT	S^2/ρ ($\mu\text{W}/\text{K}^2$ cm)	n (10^{20} cm $^{-3}$)	μ (cm $^2/\text{Vs}$)	Ref.
TiS_2	1.7	-251	67.8 (4.3)	0.16	37.1	2.8	15	this work
TiS_2 (30 K)	0.15	-87.2			52.3	3.0	133	this work
$\text{Bi}_2\text{Te}_{2.85}\text{Se}_{0.15}$	1.1	-223	15.9 (6.7)	0.85	44.8	0.4	250	23,24
$\text{Bi}_{1.65}\text{Te}_3$	1	-240	20.2 (7.4)	0.86	57.6	0.23	212	23
$\text{Sr}_8\text{Ga}_{16}\text{Ge}_{30}$	10.5	-320	8 (0.7)	0.34	9.75	0.001	2200	4,25
CoSb_3	14.2	-452	102 (0.5)	0.04	14.4	0.004	101	26
$\text{La}(\text{FeCo})\text{Sb}_3$	1.5	100	12 (4.9)	0.16	6.66	50	30	1
$\text{Yb}_{0.02}\text{Co}_4\text{Sb}_{12}$	0.6	-150	45 (12.3)	0.3	37.5			5

dence of total resistivity depends on the ratio of inter- and intra-valley scatterings, and resistivity nearly depends on T^2 when the intra- and inter-valley equally contribute to the resistivity.¹¹

Concerning large S values, the density of state above the Fermi level originated from the conduction band plays an important role. Due to the large density of state just above the Fermi level, each electron pocket could contribute to large S .^{19–22} The phonon-mediated inter-valley scattering also enhances S by giving additional scattering channels to the conduction electrons in electron pockets; that is, it increases the entropy of carriers. Besides, the strong electron-phonon coupling contributes to enhancing S by assisting the inter-valley scattering.

The power factor S^2/ρ of the TiS_2 crystal is large as shown in the inset of Fig. 4. The PF has a maximum at 52.3 $\mu\text{W}/\text{K}^2$ cm near 30 K, where the phonon-drag effect occurs. Above 50 K, the PF is almost constant, because S and ρ depend on T and T^2 , respectively, and its value at 300 K is 37.1 $\mu\text{W}/\text{K}^2$ cm. This PF is comparable to that of the best thermoelectric material, Bi_2Te_3 .

The measured in-plane and out-of-plane thermal conductivities at room temperature are 67.8 mW/K cm and 42.1 mW/K cm, respectively. The anisotropy ratio of the thermal conductivity is much smaller than that of the electrical conductivity. Because of these large thermal conductivities, the thermoelectric figure of merit is small, 0.16, at 300 K. The thermal conductivity by carriers is estimated by using the Wiedemann-Franz law to be 4.3 mW/K cm (in-plane) and 0.006 mW/K cm (out-of-plane) at 300 K. The significant difference between the measured κ and the estimated κ_e implies that most of the thermal conductivity comes from the lattice component. Thus, the anisotropy in κ corresponds to the anisotropy in κ_l , which reflects the anisotropic crystal structure of TiS_2 : that is, the TiS_6 octahedral layers provides a highly conductive phonon path in the plane, while the van der Waals gap reduces the phonon vibrations in the c direction.

It is interesting to compare the thermoelectric and transport properties of TiS_2 with those of other thermoelectric

materials.^{4,5,23–25} As listed in Table I, PF of TiS_2 at 300 K is 37.1 $\mu\text{W}/\text{K}^2$ cm, which is comparable to that of the best thermoelectric Bi_2Te_3 compound,²³ though the carrier density of TiS_2 is one order of magnitude larger than that of Bi_2Te_3 . Despite the large PF, the figure of merit ZT of TiS_2 is small, 0.16 at 300 K, because κ , 67.8 mW/K cm, is about four times larger than that of Bi_2Te_3 . However, the large κ of TiS_2 is mainly contributed by the lattice component, and this is in sharp contrast with κ of $\text{Bi}_2(\text{Te,Se})_3$, where κ_e is dominant. Hence, as found in some filled skutterudite antimonides,¹ the thermoelectric figure of merit of TiS_2 can be improved if κ_l is reduced by introducing rattling units. In CoSb_3 , by introducing heavy rattling lanthanide atoms into empty sites of the CoSb_3 cage, κ_l has been reduced by one-eighth, so ZT reaches more than unity at high temperature. In TiS_2 , various guest species, such as alkali metals, 3d transition metals, and organic molecules, can be intercalated into the van der Waals gaps.²⁷ These intercalated units weakly couple with conductive TiS_6 layers and can reduce the lattice thermal conductivity by rattling or by introducing random scattering centers. Hence, the ZT of TiS_2 can be increased. Finally, we note that PF of TiS_2 is large over a wide temperature range from 40 K to room temperature. This feature is a great advantage in applications such as very low-temperature coolers at, in particular, below liquid- N_2 temperatures.

In conclusion, by investigating transport and thermoelectric properties of “old material” TiS_2 from the viewpoint of a “new concept,” we found that TiS_2 crystal with a nearly stoichiometric composition has a large power factor, 37.1–52.3 $\mu\text{W}/\text{K}^2$ cm, which is comparable to that of the best thermoelectric, Bi_2Te_3 , over the wide temperature range. The characteristic electronic state and scattering mechanism of TiS_2 due to the two-dimensional electronic state give the significantly large power factor. Although its thermal conductivity is large compared to other thermoelectrics, most of it comes from the reducible lattice component. Thus two-dimensional metallic TiS_2 may be a good thermoelectric, when the PGEC concept is applied.

- ¹B.C. Sales, D. Mandrus, and R.K. Williams, *Science* **272**, 1325 (1996).
- ²V. Keppens, D. Madrus, B.C. Sales, B.C. Chakoumakos, P. Dai, R. Coldea, M.B. Maple, D.A. Gajewski, E.J. Freeman, and S. Bennington, *Nature (London)* **395**, 876 (1998).
- ³B.C. Sales, D. Mandrus, B.C. Chakoumakos, V. Keppens, and J.R. Thompson, *Phys. Rev. B* **56**, 15 081 (1997).
- ⁴G.S. Nolas, J.L. Cohn, G.A. Slack, and S.B. Schujman, *Appl. Phys. Lett.* **73**, 178 (1998).
- ⁵G.S. Nolas, M. Kaeser, R.T. Littleton IV, and T.M. Tritt, *Appl. Phys. Lett.* **77**, 1855 (2000).
- ⁶T. Koga, S.B. Cronin, M.S. Dresselhaus, J.L. Liu, and L. Wang, *Appl. Phys. Lett.* **77**, 1490 (2000).
- ⁷T. Yao, *Appl. Phys. Lett.* **51**, 1798 (1978).
- ⁸D.W. Song *et al.*, *Appl. Phys. Lett.* **77**, 3854 (2000).
- ⁹L.D. Hicks and M.S. Dresselhaus, *Phys. Rev. B* **47**, 12 727 (1993).
- ¹⁰C. Riekell and R. Schöllhorn, *Mater. Res. Bull.* **10**, 629 (1975).
- ¹¹P.C. Klipstein, A.G. Baganall, W.Y. Liang, E.A. Marseglia, and R.H. Friend, *J. Phys. C* **14**, 4067 (1981).
- ¹²C. Julien, I. Samaras, O. Gorochoy, and A.M. Ghorayeb, *Phys. Rev. B* **45**, 13 390 (1992).
- ¹³M. Inoue, H. Negishi, T. Fujii, K. Takase, Y. Hara, and M. Sasaki, *J. Phys. Chem. Solids* **57**, 1109 (1996).
- ¹⁴M. Inoue, M. Koyano, H. Negishi, Y. Ueda, and H. Sato, *Phys. Status Solidi B* **132**, 295 (1985).
- ¹⁵C.A. Kukkonen, W.J. Kaiser, E.M. Logothetis, B.J. Blumenstock, P.A. Schroeder, S.P. Faile, R. Colella, and J. Gambold, *Phys. Rev. B* **24**, 1691 (1981).
- ¹⁶P.C. Klipstein and R.H. Friend, *J. Phys. C* **17**, 2713 (1984).
- ¹⁷R. D. Barnard, in *Thermoelectricity in Metals and Alloys* (Taylor & Francis, London, 1972).
- ¹⁸M. Koyano, H. Negishi, Y. Ueda, M. Sasaki, and M. Inoue, *Phys. Status Solidi B* **138**, 357 (1986).
- ¹⁹Z.Y. Wu, F. Lemoigno, P. Gressier, G. Ouvrard, P. Moreau, J. Rouxel, and C.R. Natoli, *Phys. Rev. B* **54**, 11 009 (1996).
- ²⁰S. Sharma, T. Nautiyal, G.S. Singh, S. Auluck, P. Blaha, and C. Ambrosch-Draxl, *Phys. Rev. B* **59**, 14 833 (1999).
- ²¹M.-L. Doublet, N. Gallego-Planas, P.H.T. Philipsen, R. Brec, and S. Jobic, *J. Chem. Phys.* **108**, 649 (1998).
- ²²Y. Shimakawa (unpublished).
- ²³H. Scherrer and S. Scherrer, in *CRC Handbook of Thermoelectrics*, edited by D. M. Rowe (CRC, Boca Raton, FL, 1995), p. 211, and references therein.
- ²⁴G. S. Nolas, J. W. Sharp, and H. J. Goldsmid, in *Thermoelectrics: Basic Principles and New Materials Developments* (Springer-Verlag, Heidelberg, 2001).
- ²⁵G. S. Nolas, G. A. Slack, and S. B. Schujman, in *Semiconductors and Semimetals*, edited by T. M. Tritt (Academic Press, New York, 2000), Vol. 69, p. 255.
- ²⁶T. Caillat, A. Borshevsky, and J.-P. Fleurial, *J. Appl. Phys.* **80**, 4442 (1996).
- ²⁷For examples, W. M. Warmuth and R. Rchöllhorn, in *Progress in Intercalation Research* (Kluwer Academic Publ., Dordrecht, 1994).